Supporting information for

Use of heterometallic alkali metal-magnesium aryloxides in ring-opening polymerization of cyclic esters

Rafał Petrus,[a,*] Tadeusz Lis[b], Adrian Kowaliński[a]

[a]Faculty of Chemistry, Wrocław University of Science and Technology, 23 Smoluchowskiego, 50-370 Wrocław, Poland

[b]Faculty of Chemistry, University of Wrocław, 14 F. Joliot-Curie, 50-383 Wrocław, Poland

Corresponding author:
Dr. Rafał Petrus, rafal.petrus@pwr.edu.pl

Contents

Crystallographic Data for Compounds 4-8.

Table S1. Crystal and data collection parameters for compounds **4**-**8**.

Crystal	**4**	**5**	**6**·(C_4H_8O)	**7**·2(C_4H_8O)	**8**
Chemical formula	$C_{54}H_{54}Li_2Mg_2O_{18}$	$C_{27}H_{27}KMgO_9$	$C_{118}H_{118}AlMg_6Na_4O_{50}$	$C_{86}H_{98}Mg_4Na_2O_{30}$	$C_{40}H_{56}Mg_4O_{20}$
Formula Mass	1053.47	558.89	2600.92	1754.86	954.08
Crystal system	Monoclinic	Triclinic	Monoclinic	Monoclinic	Tetragonal
Space group	$P2_1/n$	$P1$	$C2/c$	$P2_1/n$	$I4_1/a$
a/Å	11.669 (2)	6.610 (2)	58.522 (18)	17.285 (3)	15.850 (3)
b/Å	17.376 (3)	12.874 (4)	15.832 (5)	13.750 (3)	
c/Å	13.155 (2)	16.166 (5)	27.991 (12)	18.986 (4)	18.016 (3)
α/°		97.48 (4)			
β/°	92.27 (2)	90.45 (4)	108.43 (5)	106.54 (2)	
γ/°		97.24 (4)			
Unit cell volume/Å^3	2665.2 (8)	1352.7 (7)	24604 (17)	4325.7 (16)	4526.0 (19)
Temperature/K	100(2)	100(2)	100(2)	100(2)	100(2)
Z	2	2	8	2	4
Radiation type	MoKα	MoKα	MoKα	MoKα	MoKα
Absorption coefficient, μ/mm^{-1}	0.12	0.27	0.15	0.14	0.16
No. of reflections measured	27574	14609	54054	41380	5798
No. of independent reflections	5802	14609	24832	10372	2436
No. of observed reflections ($I > 2\sigma(I)$)	5127	9709	8570	6235	1946
R_{int}	0.0390	-	0.0948	0.0801	0.0784
Final R_1 values ($I > 2\sigma(I)$)	0.0422	0.0727	0.0782	0.0480	0.0775
Final $wR(F^2)$ values ($I > 2\sigma(I)$)	0.1122	0.1594	0.1564	0.1118	0.1980
Final R_1 values (all data)	0.0477	0.1130	0.2219	0.0855	0.0916
Final $wR(F^2)$ values (all data)	0.1188	0.1594	0.2427	0.1215	0.2126
Goodness of fit on F^2	1.032	0.97	0.98	0.87	1.09
Δρmax/eÅ^{-3}	0.35	0.51	0.82	0.49	0.77
Δρmin/eÅ^{-3}	-0.25	-0.57	-0.44	-0.51	-0.67

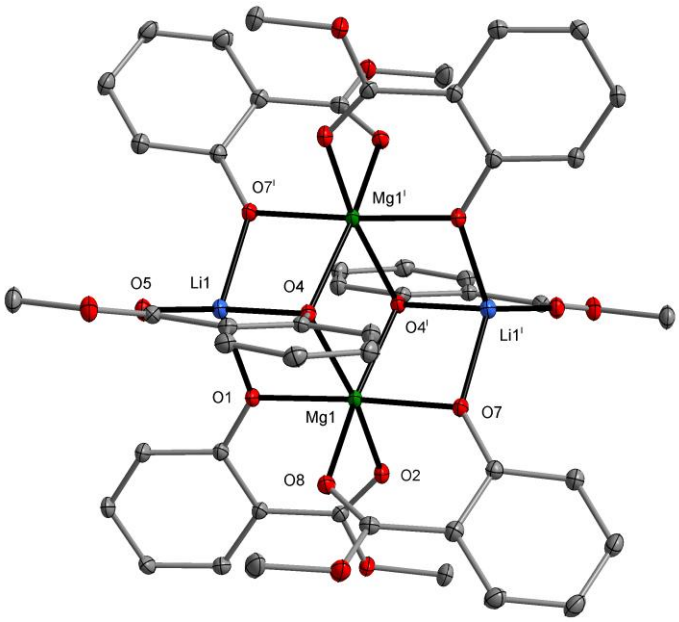

Figure S1. Molecular structure of $[Mg_2Li_2(MesalO)_6]$ (**1**) with displacement ellipsoids drawn at the 25% probability level. Hydrogen atoms are omitted for clarity [symmetry code: (i) −x+1, −y+1, −z+1]. Reprinted (adapted) with permission from *Macromolecules* 2021, 54, 5, 2449–2465. Copyright 2021 American Chemical Society.

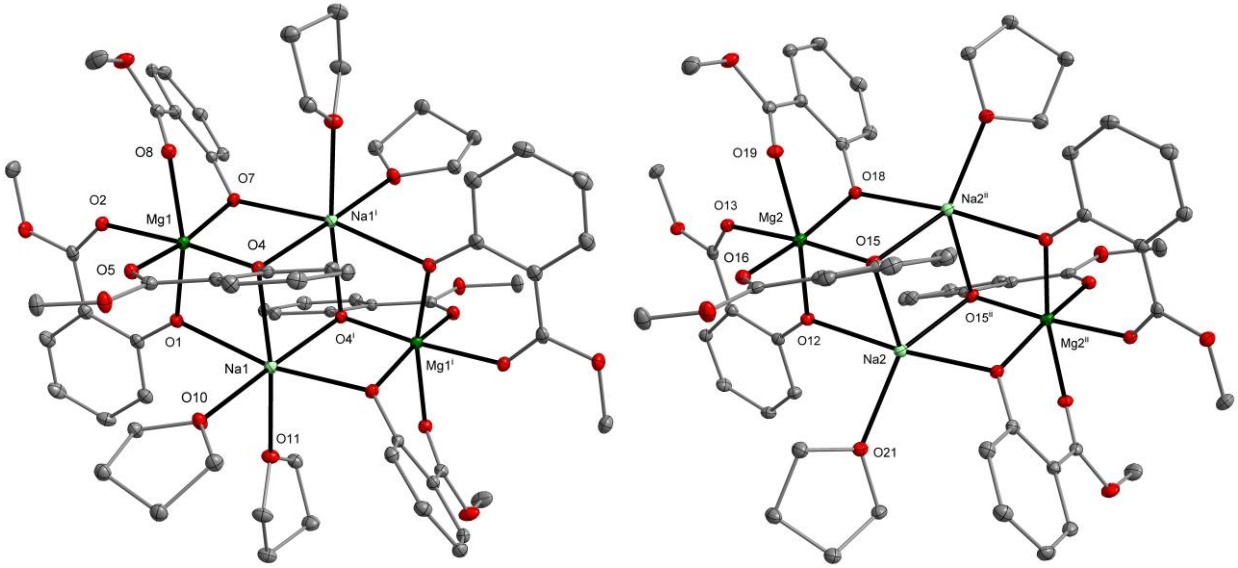

Figure S2. Molecular structure of $[Mg_2Na_2(MesalO)_6(THF)_y]$ (**2**) for y = 2 or 4 with displacement ellipsoids drawn at the 25% probability level. The hydrogen atoms are omitted for clarity [symmetry code: (i) −x+1, −y+1, −z+1; (ii) −x, −y, −z]. Reprinted (adapted) with permission from *Macromolecules* 2021, 54, 5, 2449–2465. Copyright 2021 American Chemical Society.

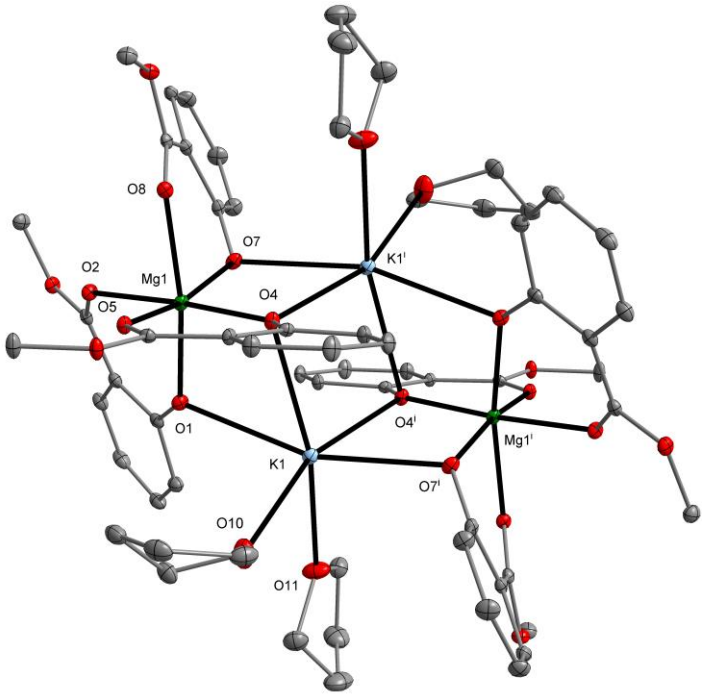

Figure S3. Molecular structure of $[Mg_2K_2(MesalO)_6(THF)_4]$ (**3**) with displacement ellipsoids drawn at the 25% probability level. The hydrogen atoms are omitted for clarity [symmetry code: (i) −x+1, −y+1, −z+1]. Reprinted (adapted) with permission from *Macromolecules* 2021, 54, 5, 2449–2465. Copyright 2021 American Chemical Society.

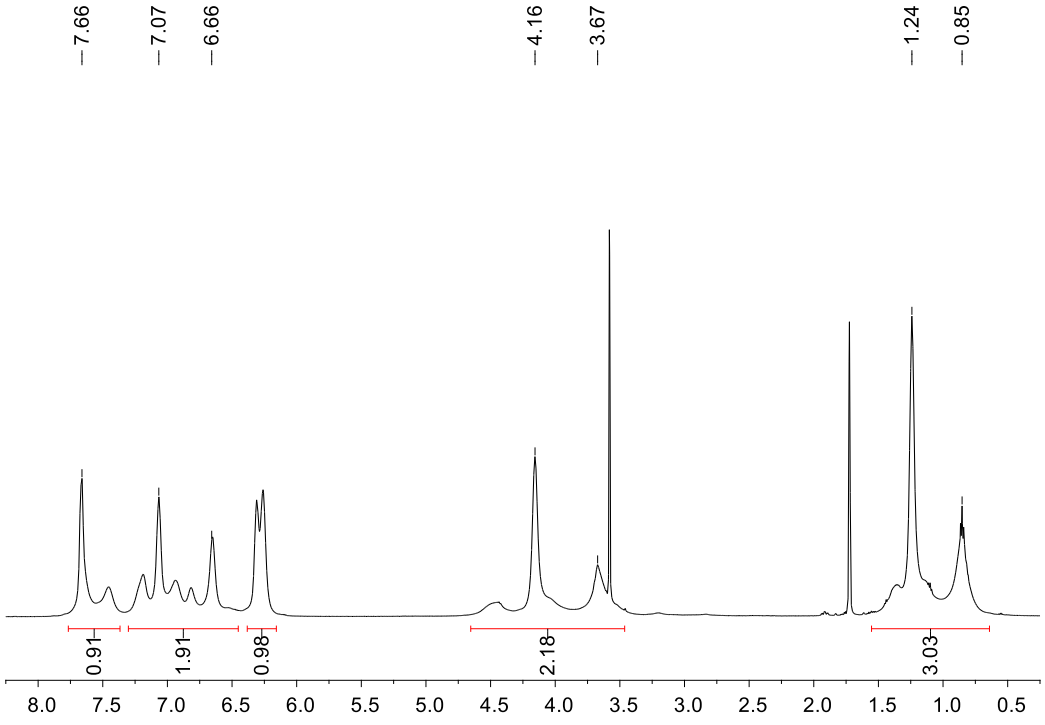

Figure S4. ^{1}H NMR spectrum of **4** in THF-d_8.

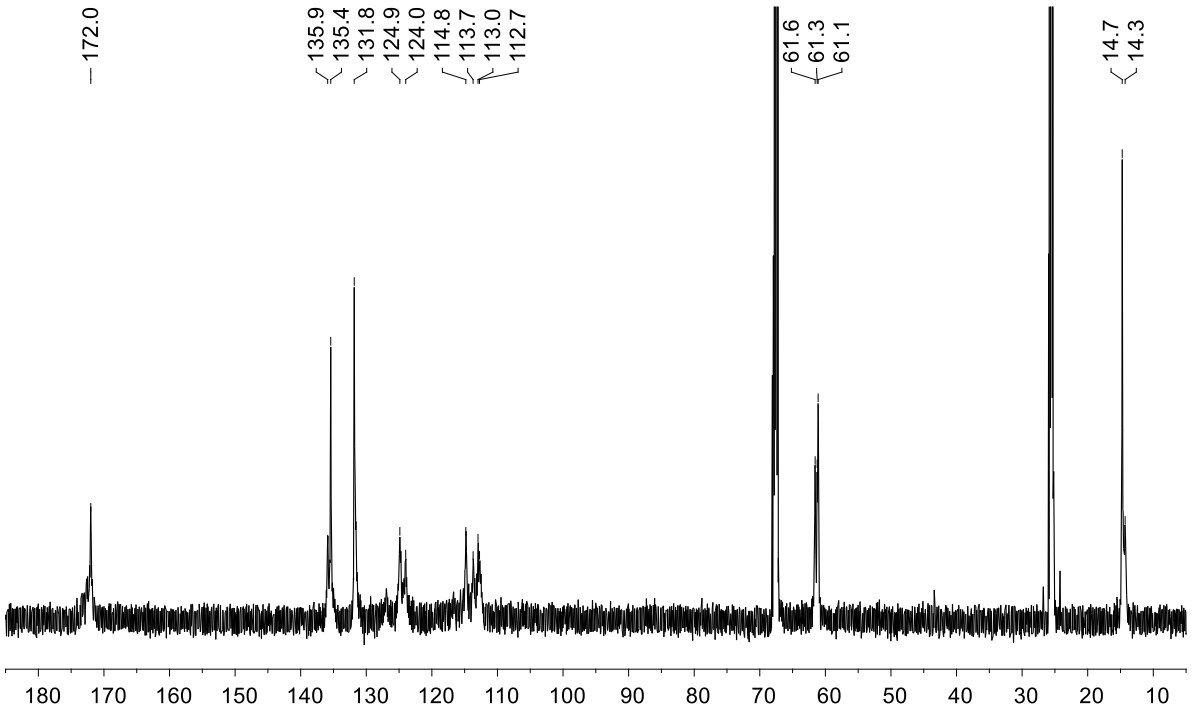

Figure S5. $^{13}C\{^{1}H\}$ NMR spectrum of **4** in THF-d_8.

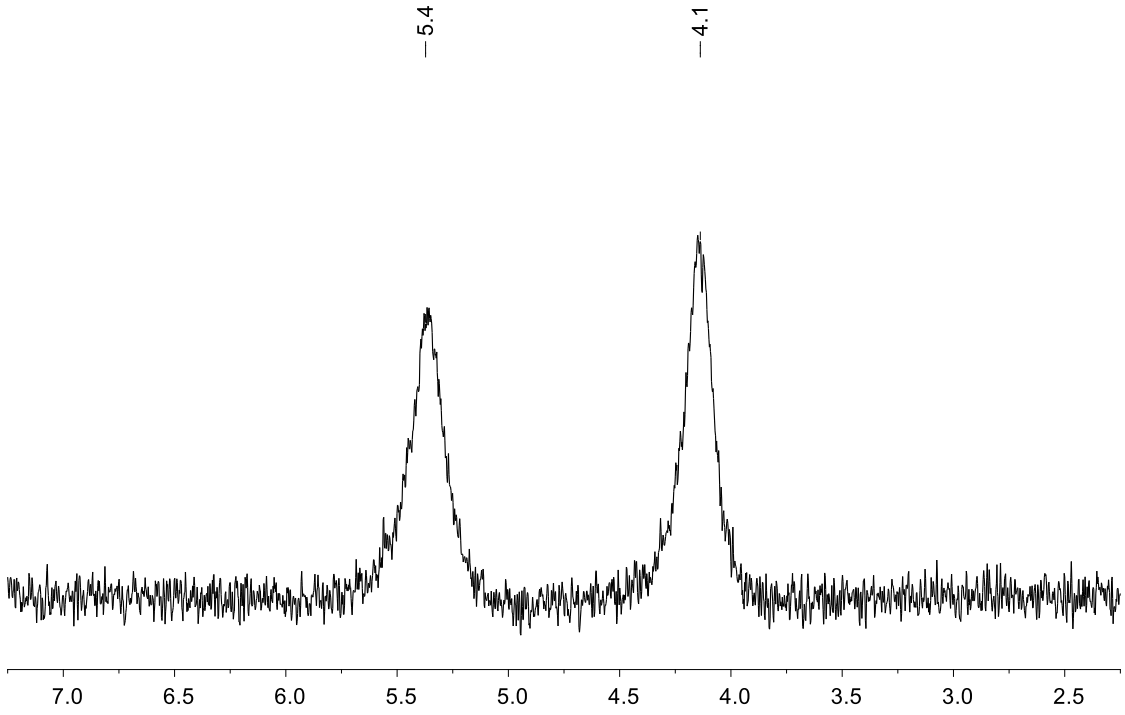

Figure S6. ^{7}Li NMR spectrum of **4** in THF-d_8.

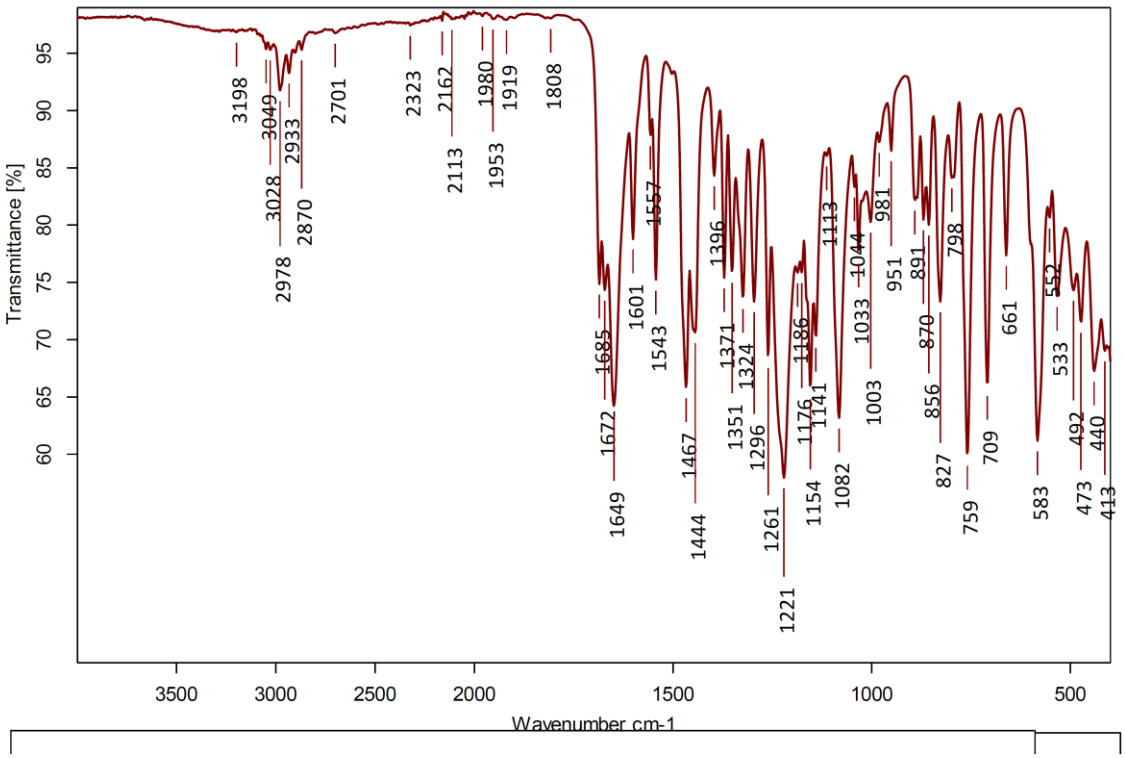

Figure S7. FTIR-ATR spectrum of **4**.

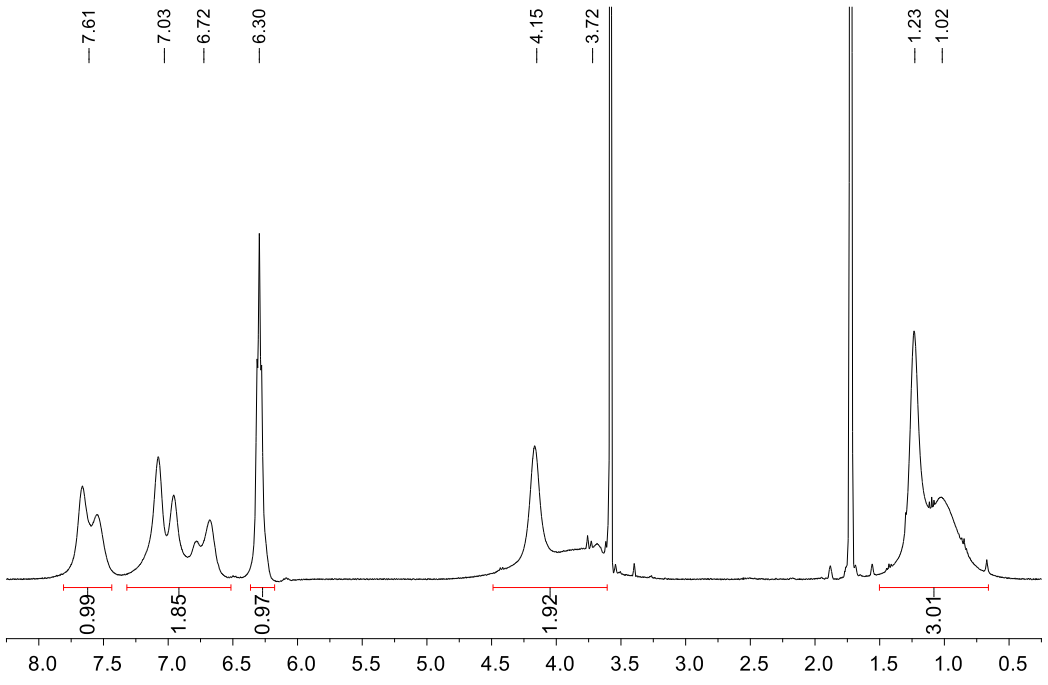

Figure S8. ^{1}H NMR spectrum of **4** in THF-d_8 at 50 °C.

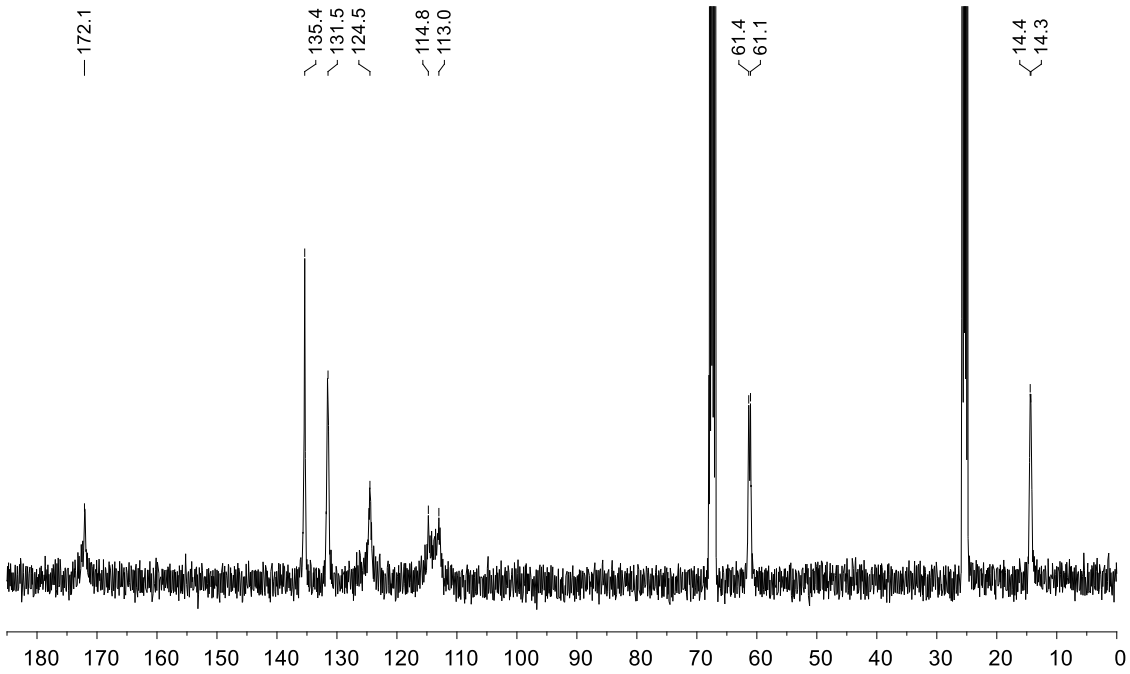

Figure S9. $^{13}C\{^{1}H\}$ NMR spectrum of **4** in THF-d_8 at 50 °C.

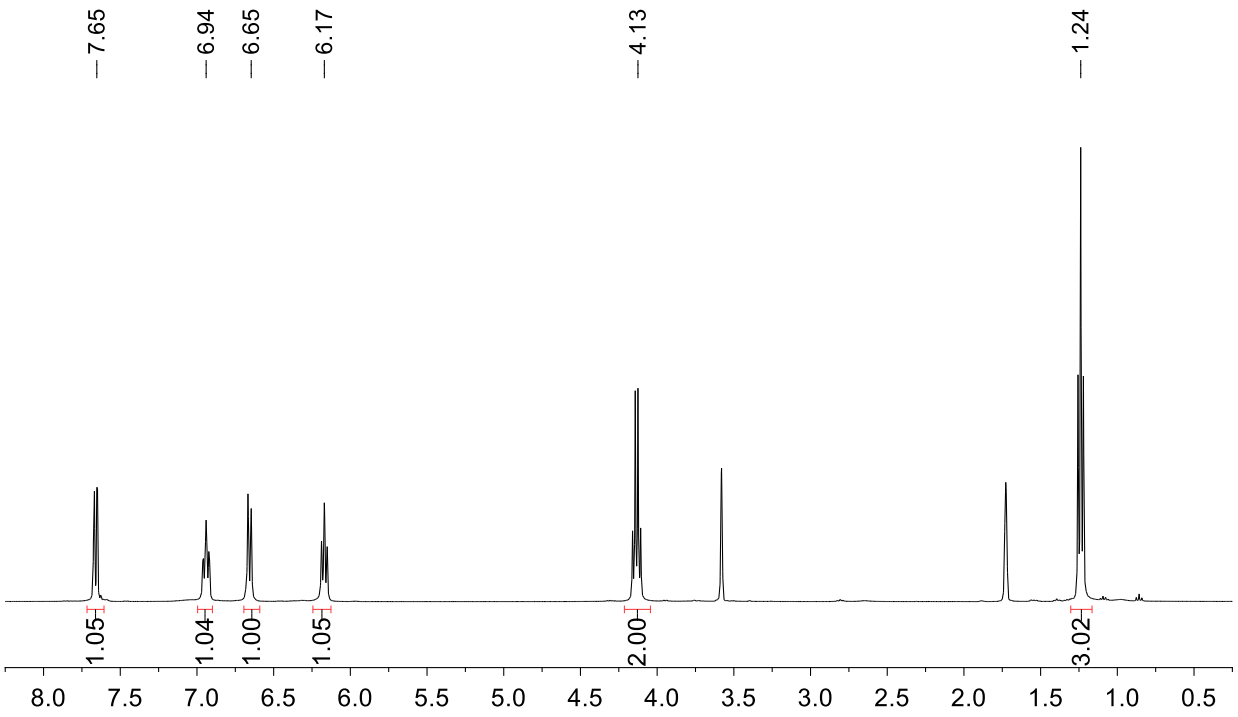

Figure S10. ^{1}H NMR spectrum of **5** in THF-d_8.

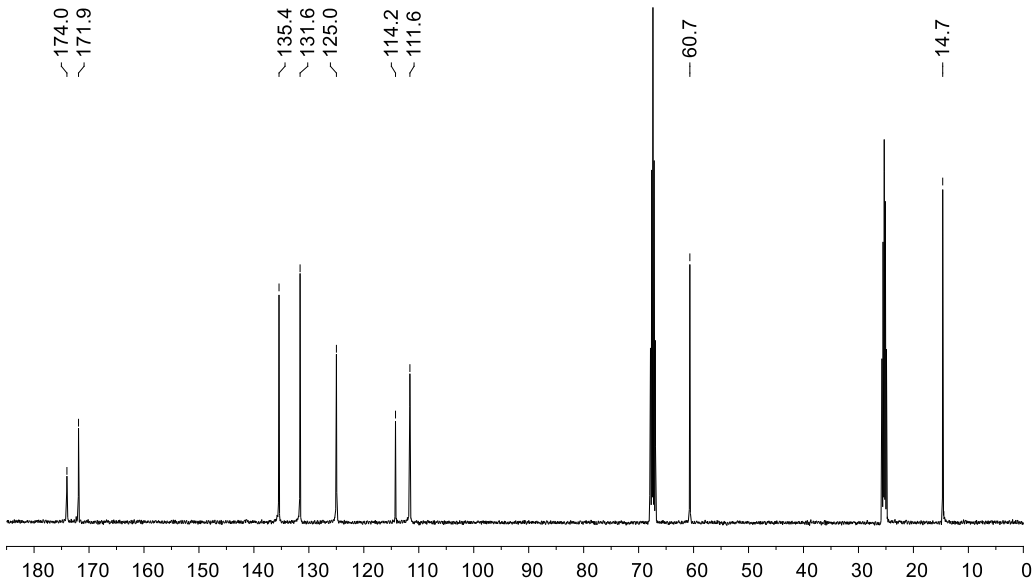

Figure S11. $^{13}C\{^{1}H\}$ NMR spectrum of **5** in THF-d_8.

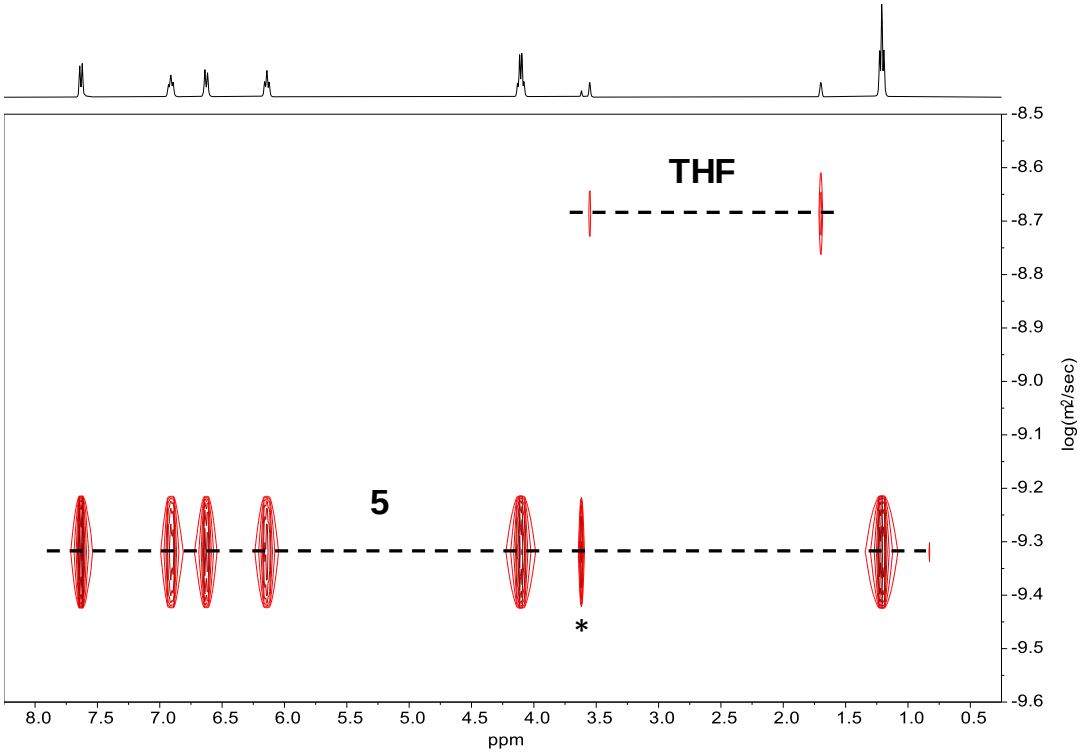

Figure S12. ^{1}H-DOSY NMR spectrum of **5** in THF-d_8. * - assigned the residues of MesalO ligands.

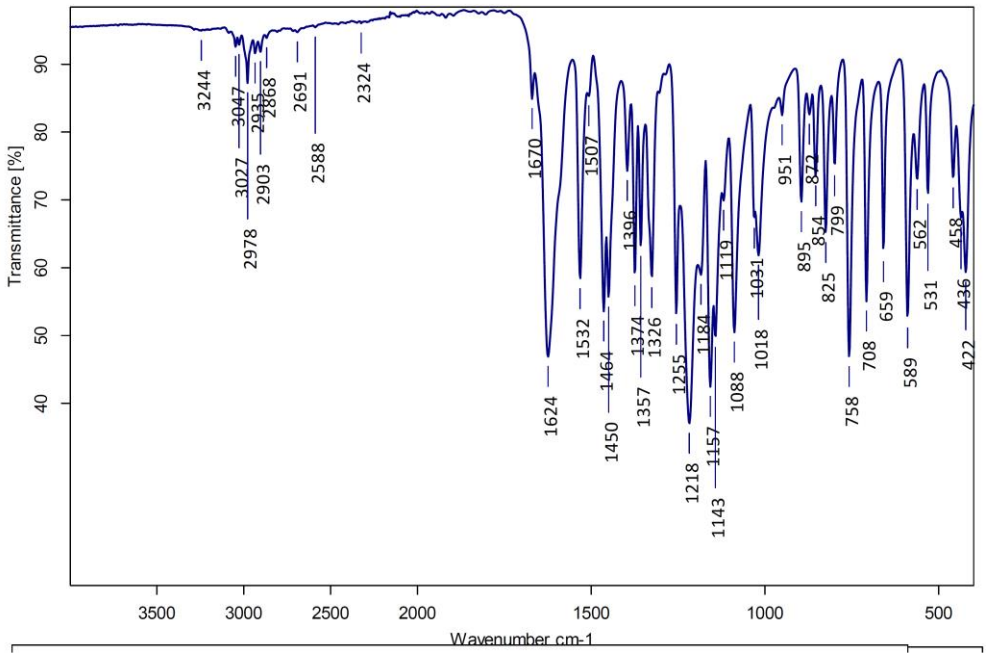

Figure S13. FTIR-ATR spectrum of **5**.

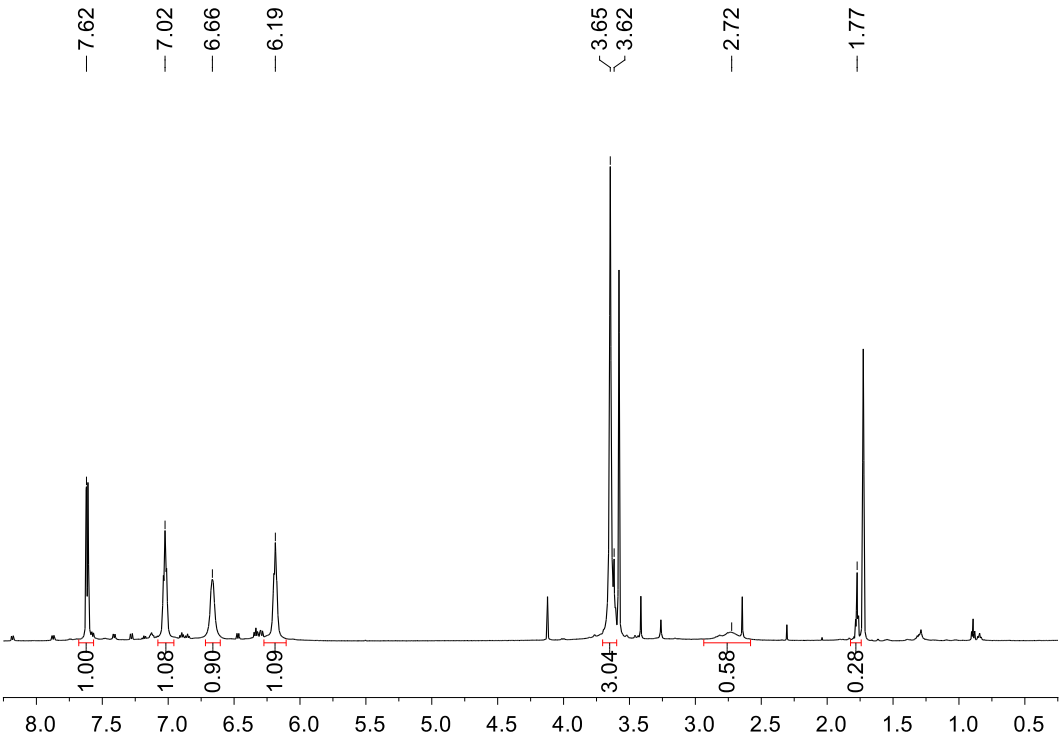

Figure S14. ^{1}H NMR spectrum of **6** in THF-d_8.

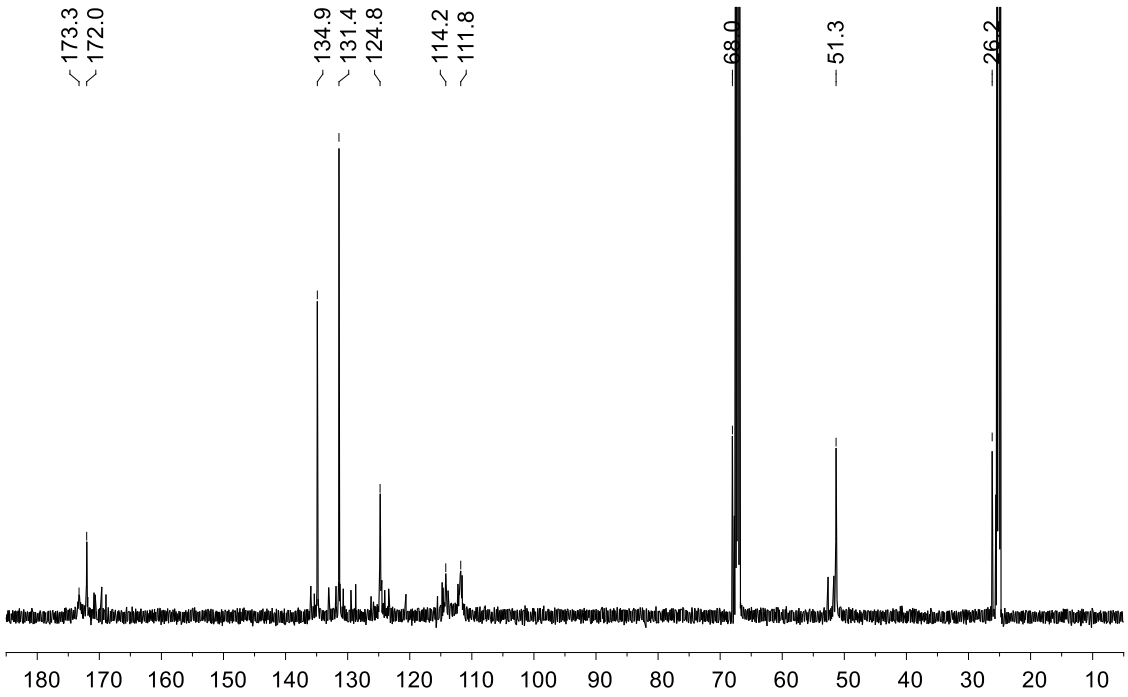

Figure S15. $^{13}C\{^{1}H\}$ NMR spectrum of **6** in THF-d_8.

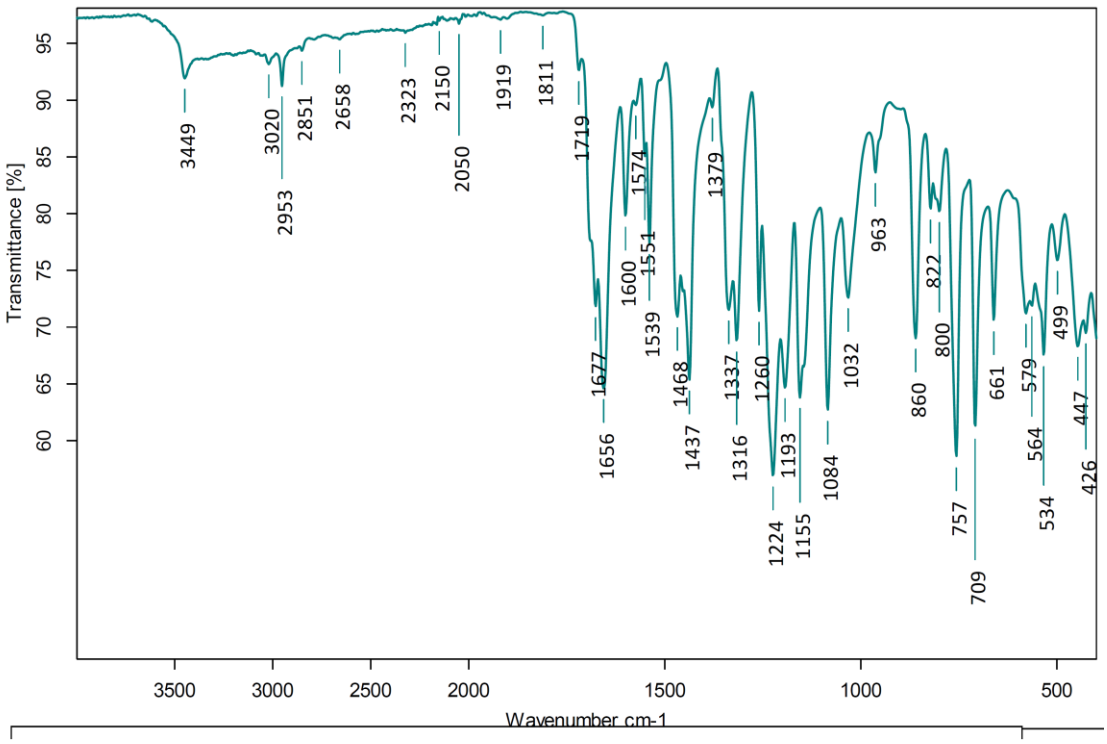

Figure S16. FTIR-ATR spectrum of **6**.

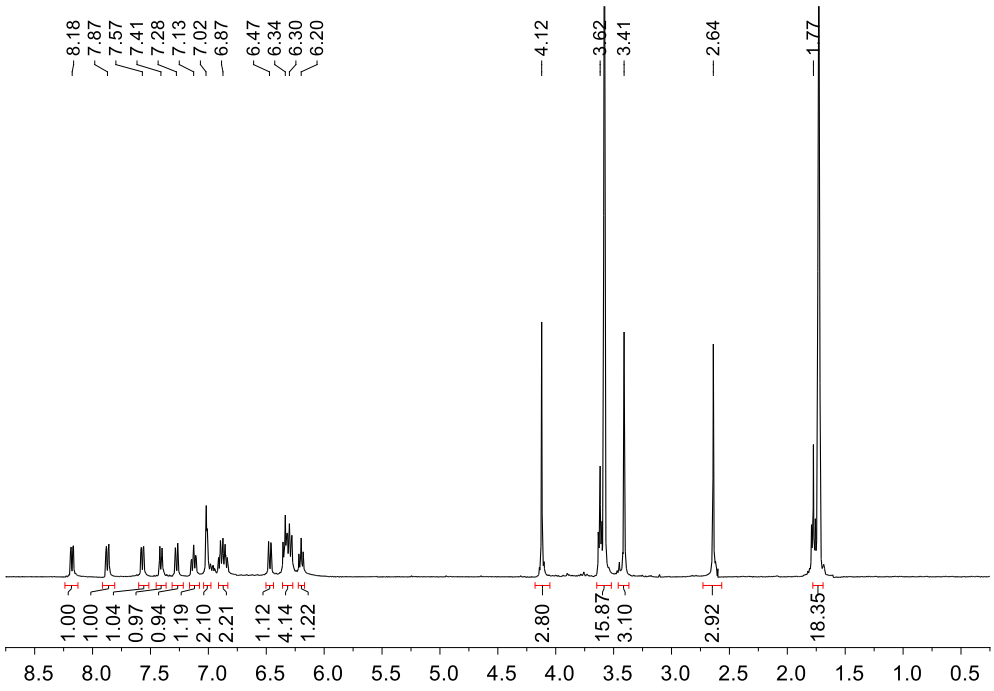

Figure S17. ^{1}H NMR spectrum of **7** in THF-d_8.

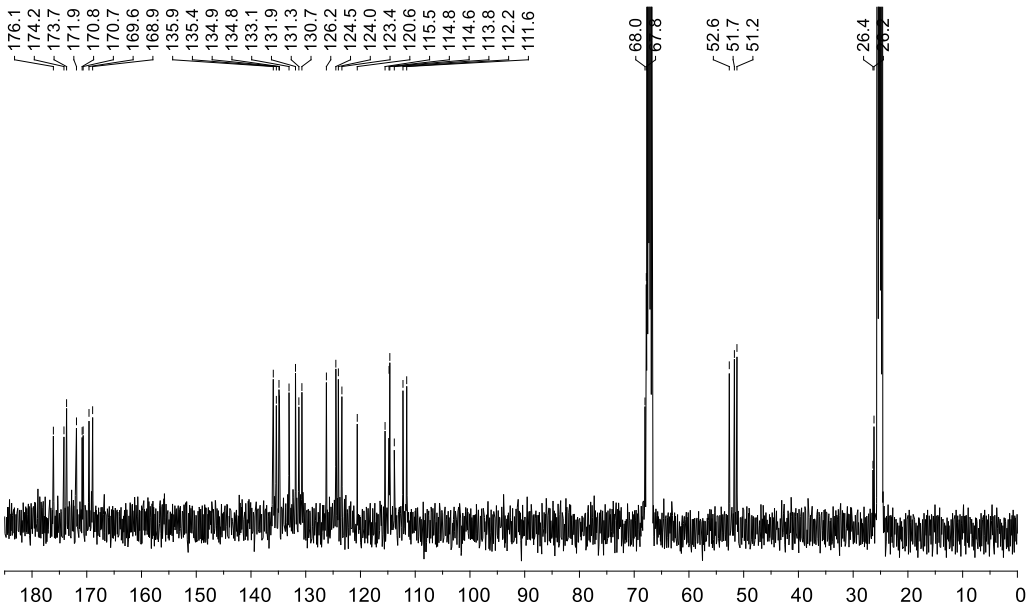

Figure S18. ^{13}C{^{1}H} NMR spectrum of **7** in THF-d_8.

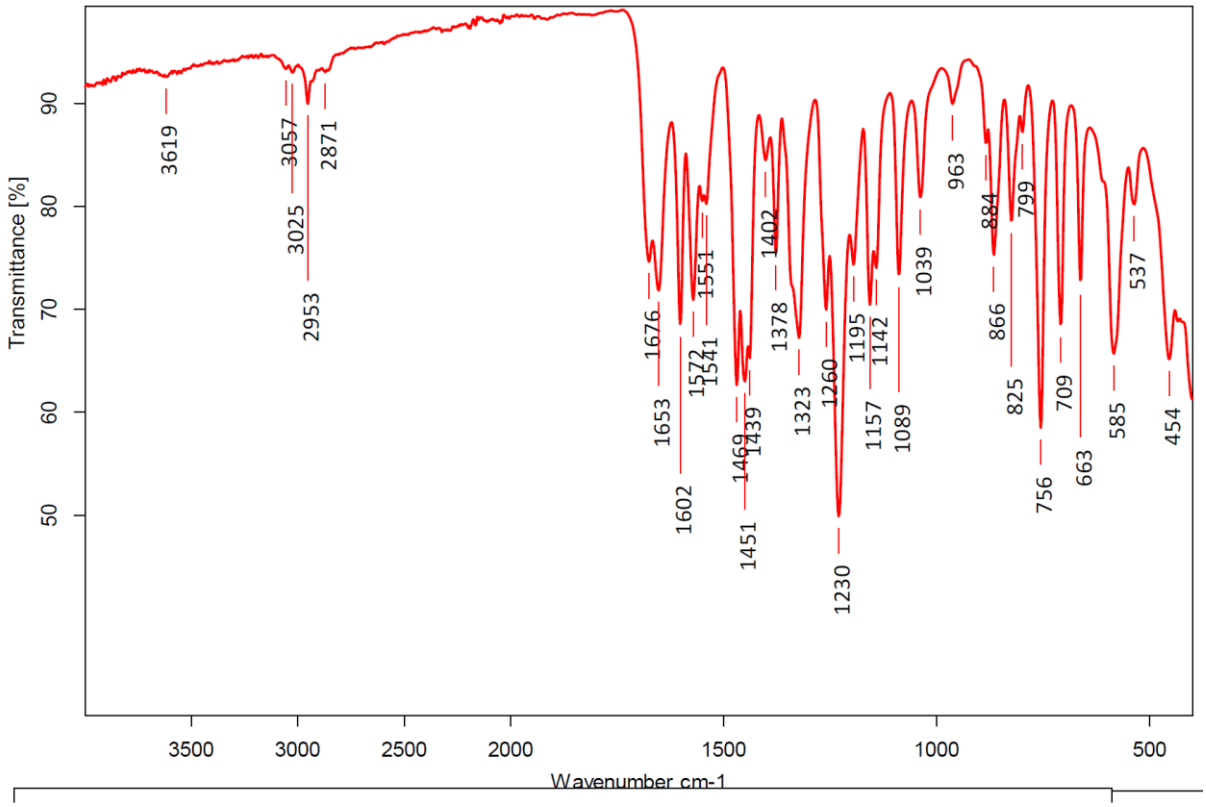

Figure S19. FTIR-ATR spectrum of **7**.

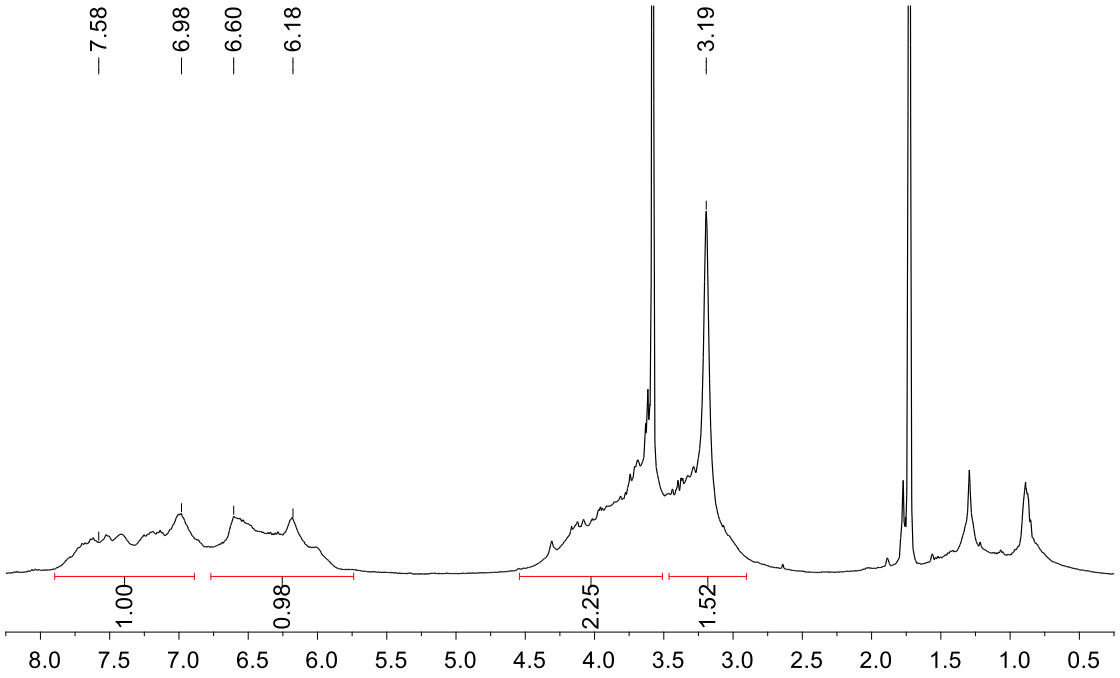

Figure S20. ^{1}H NMR spectrum of **8** in THF-d_8.

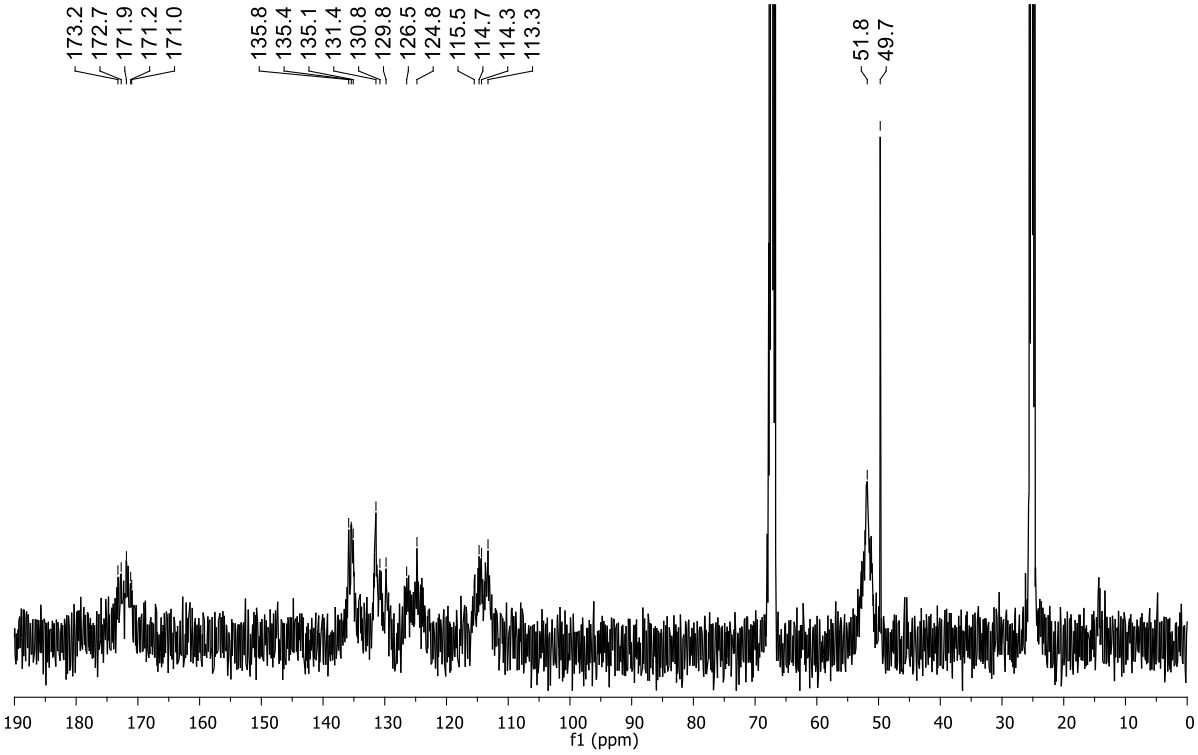

Figure S21. ^{13}C NMR spectrum of **8** in THF-d_8.

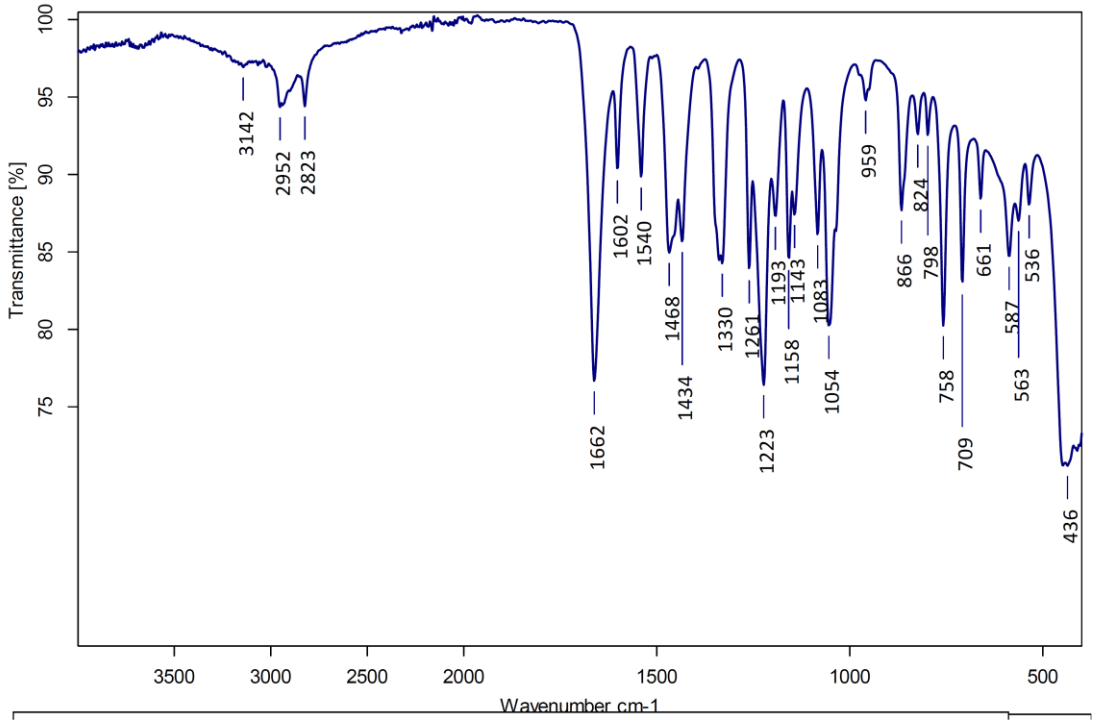

Figure S22. FTIR-ATR spectrum of **8**.

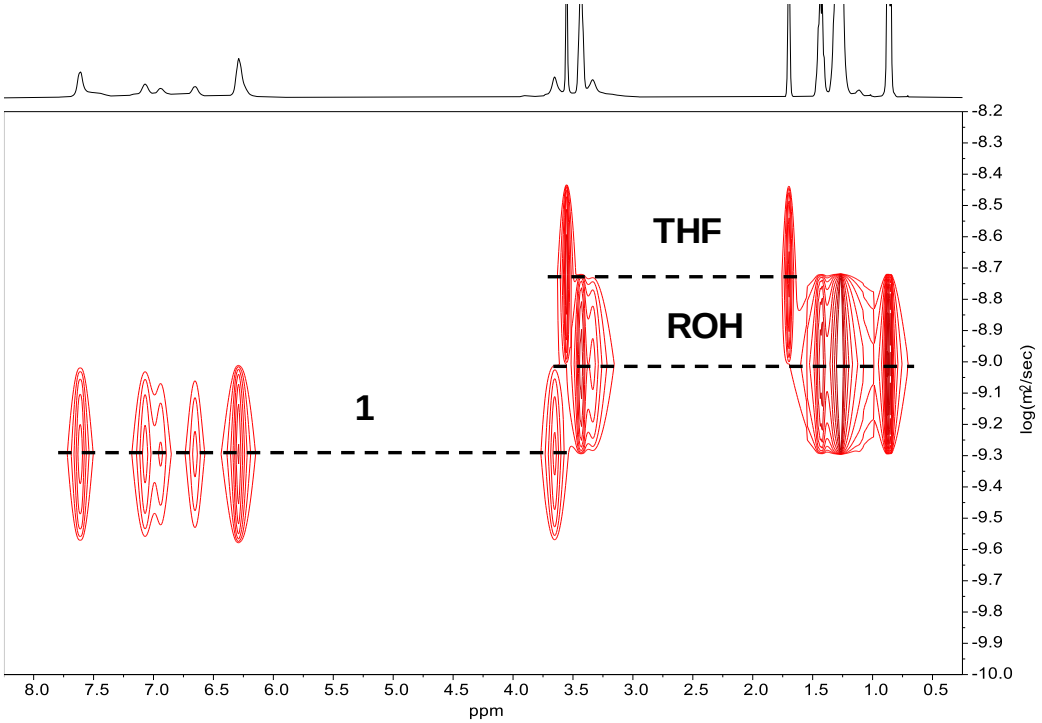

Figure S23. ^{1}H-DOSY NMR spectrum of the mixture of **1** and 4 equiv. of cetyl alcohol in THF-d_8.

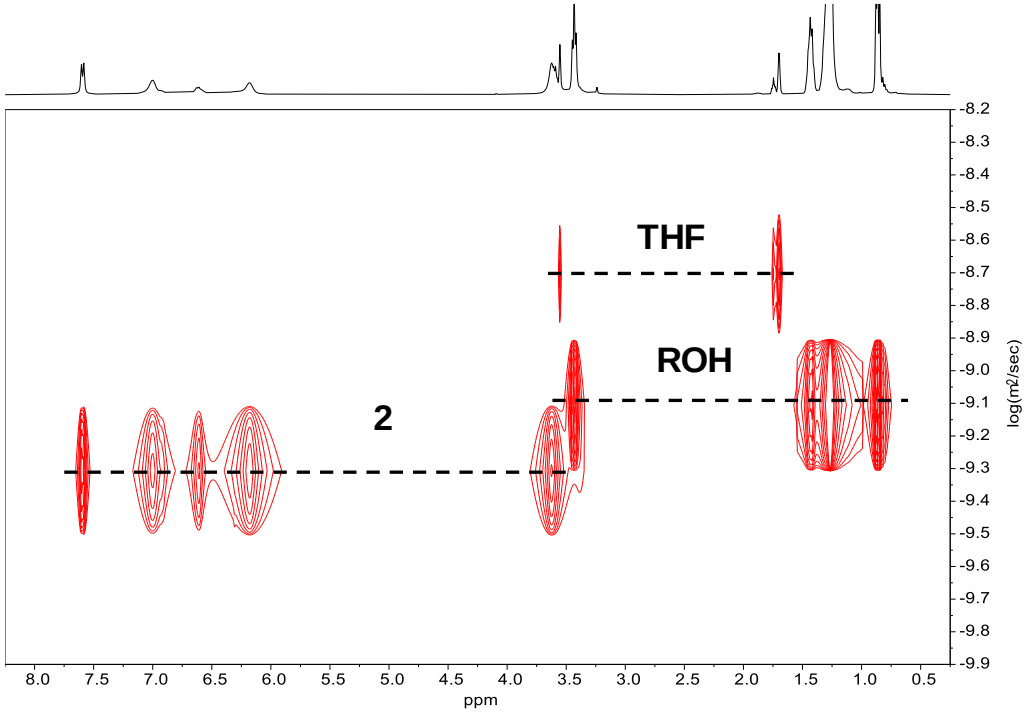

Figure S24. ^{1}H-DOSY NMR spectrum of the mixture of **2** and 4 equiv. of cetyl alcohol in THF-d_8.

Table S2. Formula weights (Fws) and the hydrodynamic radii (r_H) of **1**-**3** and **5** estimated from Stokes-Einstein Gierer-Wirtz method.

compound	log($D_{x,norm}$)	Fw (g/mol)	Fw_{calc} (g/mol)	$r_{x\text{-}ray}$ (Å)	r_H (Å)	Δ Fw (%)
1	-9.168	969	944	6.82	8.42	3
2	-9.216	1290	1214	7.23	9.16	6
3	-9.236	1322	1354	7.24	9.49	2
1	-9.234	969	1060	6.82	8.75	9
2	-9.232	1290	1264	7.23	9.28	2
3	-9.236	1322	1302	7.24	9.37	2
5	-9.258	1406	1519	6.86	9.86	7

Table S3. Diffusion coefficients and estimated formula weight for **1**-**3** and **6**-**7** determine using calibration plots.

compound	log(D_x)	Fw (g/mol)	Fw_{calc} (g/mol)	Δ Fw (%)
1	-9.200	969	1156	19
2	-9.230	1290	1273	2
3	-9.290	1322	1516	15
7	-9.233	1610	2035	26
6	-9.238 (**2**)	1290	1107	14
	-9.333 (**7**)	1610	1702	6
	-9.436	2556	2710	6

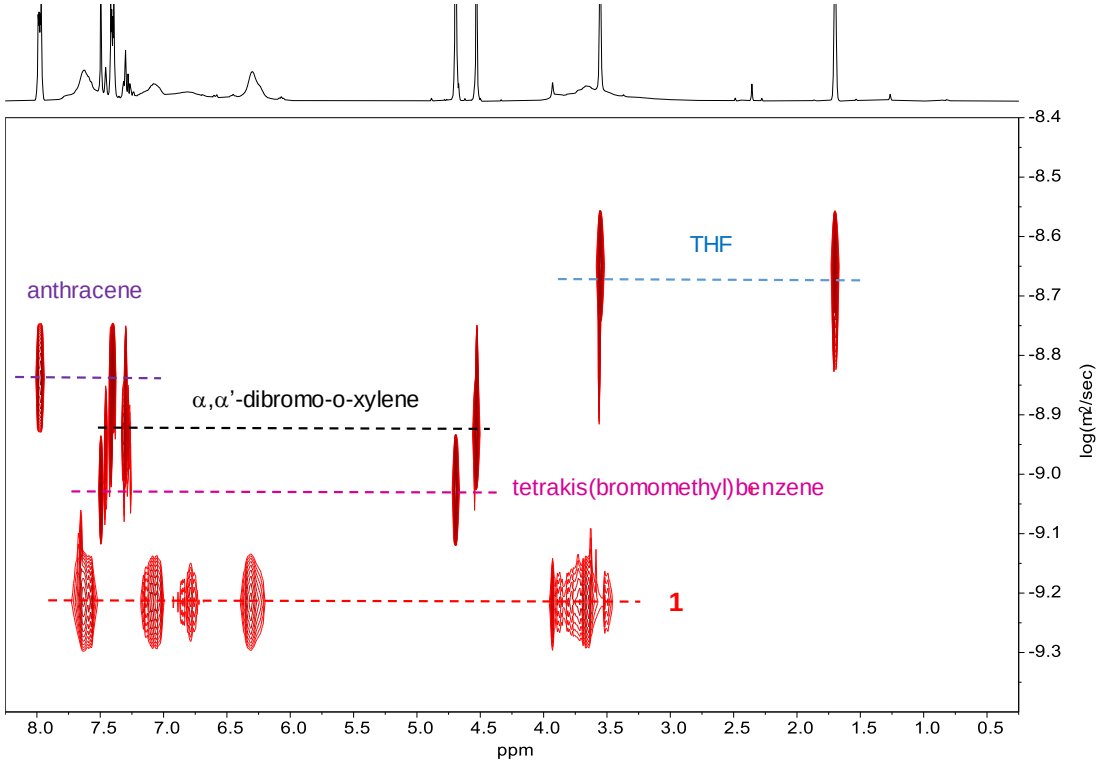

Figure S25. ^{1}H DOSY NMR spectrum of a mixture of anthracene, α,α'-dibromo-o-xylene, 1,2,4,5-tetrakis(bromomethyl)benzene, and **1** in THF-d_8.

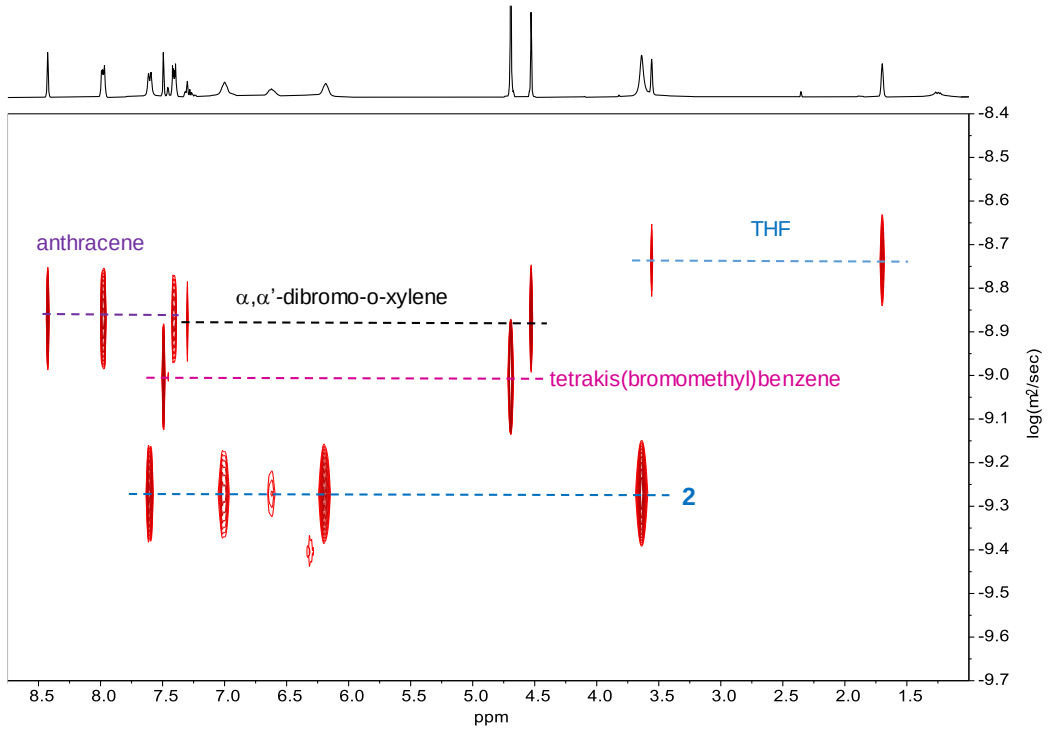

Figure S26. ^{1}H DOSY NMR spectrum of a mixture of anthracene, α,α'-dibromo-o-xylene, 1,2,4,5-tetrakis(bromomethyl)benzene, and **2** in THF-d_8.

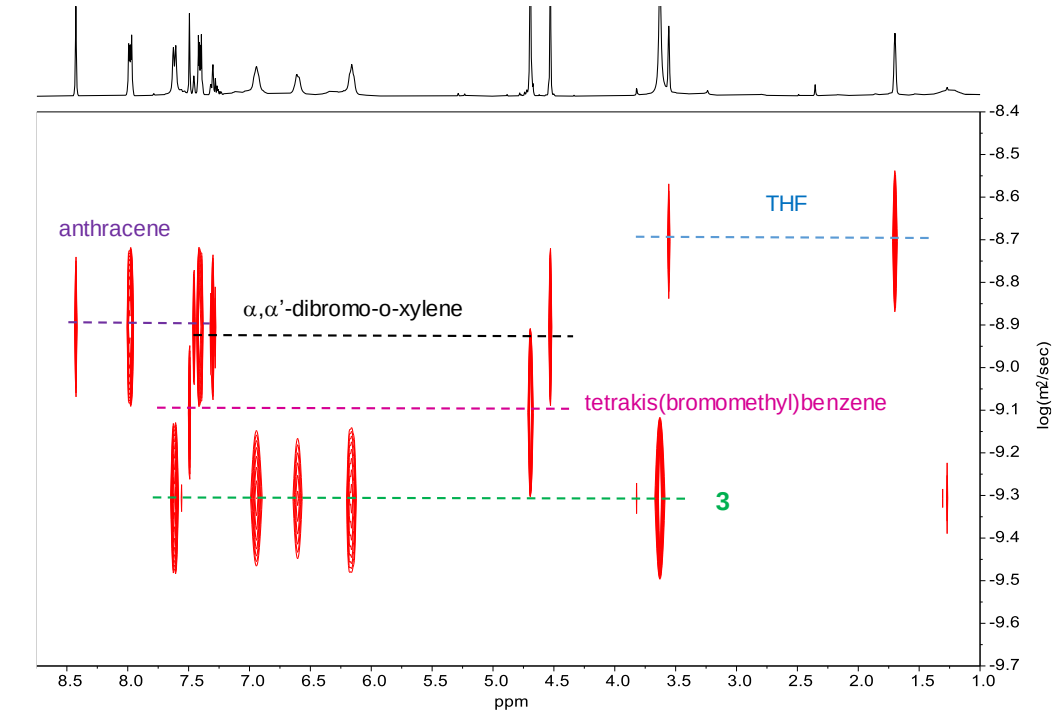

Figure S27. ^{1}H DOSY NMR spectrum of a mixture of anthracene, α,α'-dibromo-o-xylene, 1,2,4,5-tetrakis(bromomethyl)benzene, and **3** in THF-d_8.

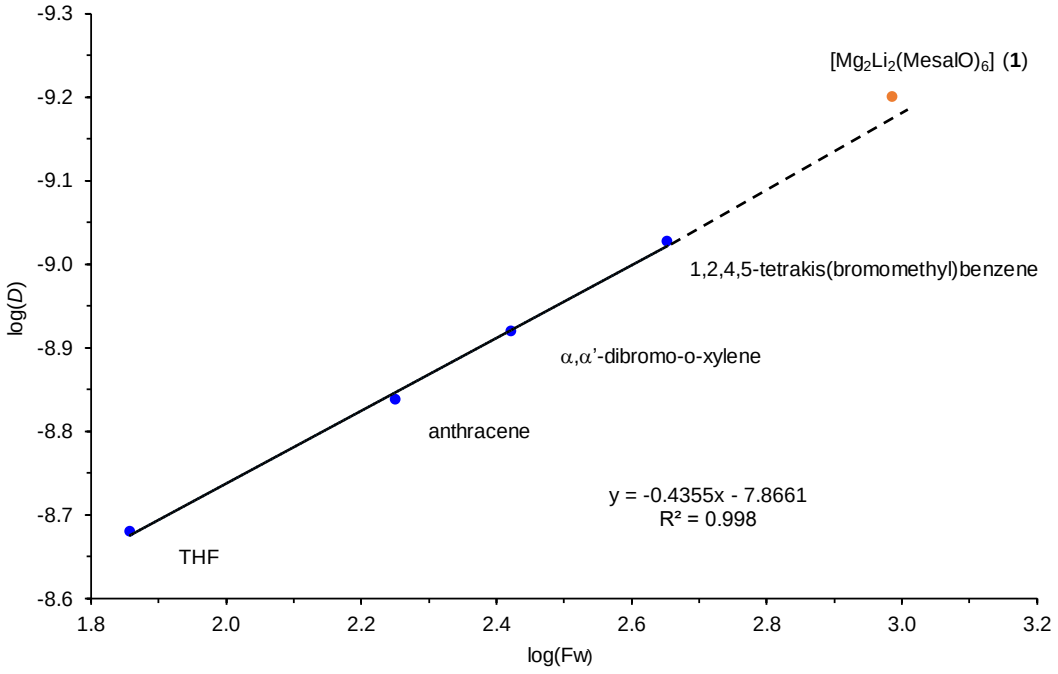

Figure S28. Plot of diffusion coefficient (log*D*) versus formula weight (log Fw) of a mixture of anthracene, α,α'-dibromo-o-xylene, 1,2,4,5-tetrakis(bromomethyl)benzene and **1** in THF-d_8.

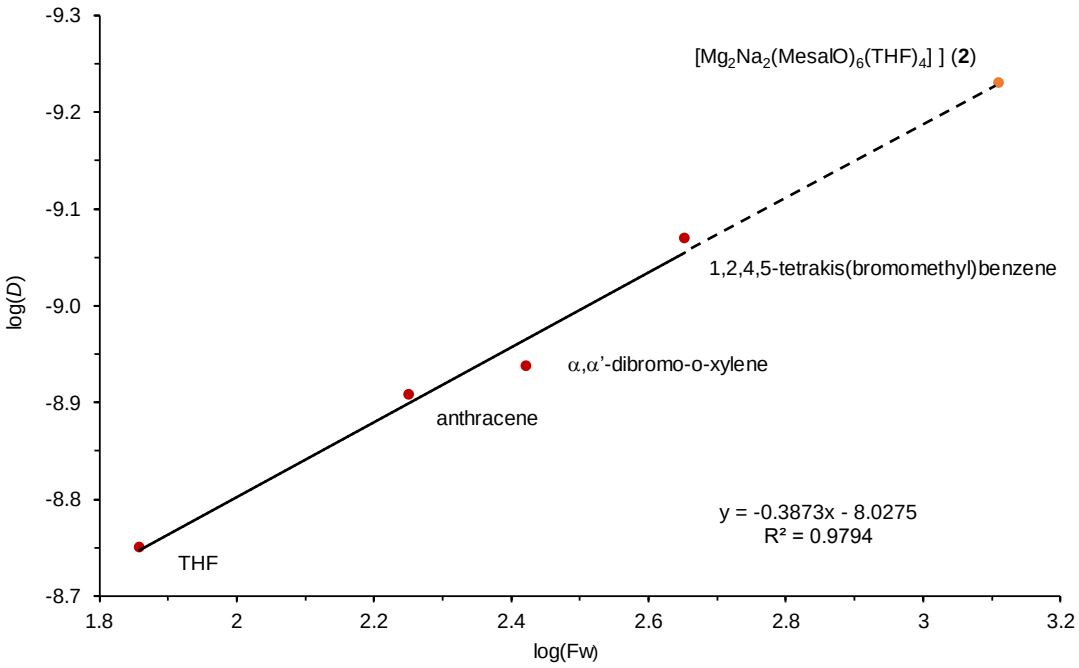

Figure S29. Plot of diffusion coefficient (log*D*) versus formula weight (log Fw) of a mixture of anthracene, α,α'-dibromo-o-xylene, 1,2,4,5-tetrakis(bromomethyl)benzene and **2** in THF-d_8.

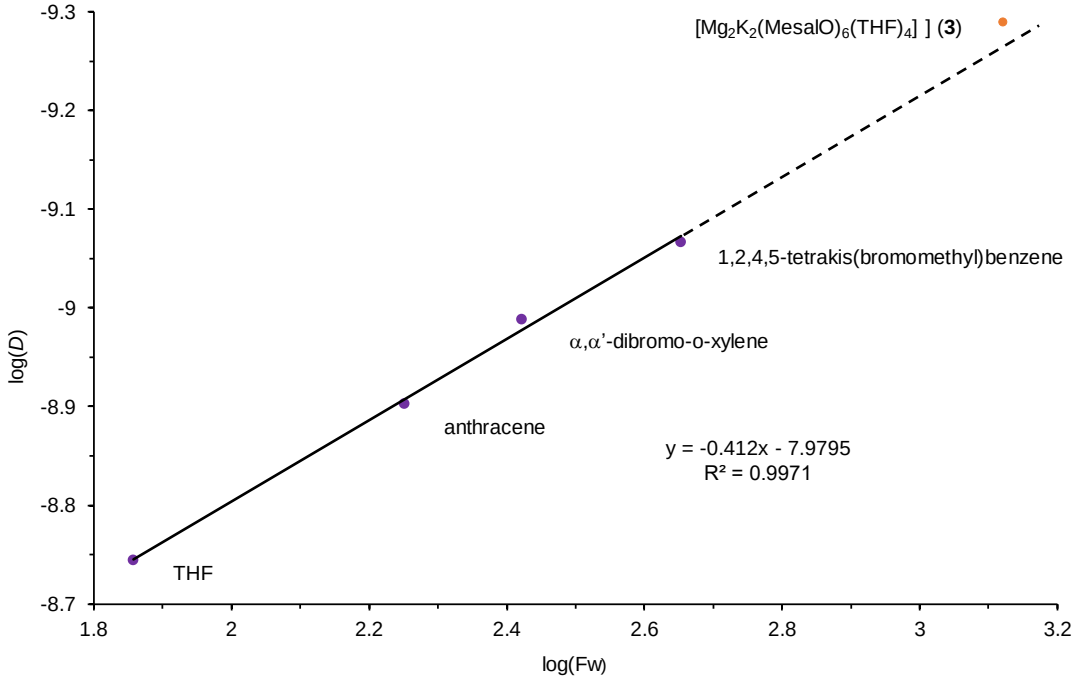

Figure S30. Plot of diffusion coefficient (log*D*) versus formula weight (log Fw) of a mixture of anthracene, α,α'-dibromo-o-xylene, 1,2,4,5-tetrakis(bromomethyl)benzene and **3** in THF-d_8.

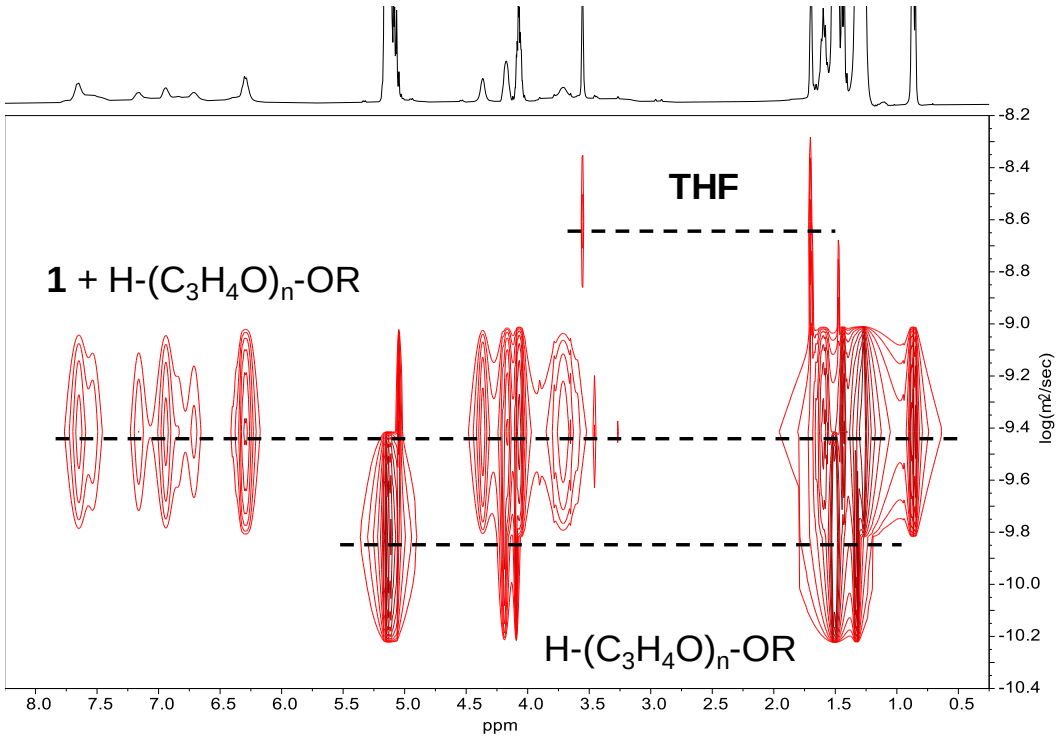

Figure S31. ^{1}H-DOSY NMR spectrum in THF-d_8 of the PLLA synthesized using **1** and ROH.

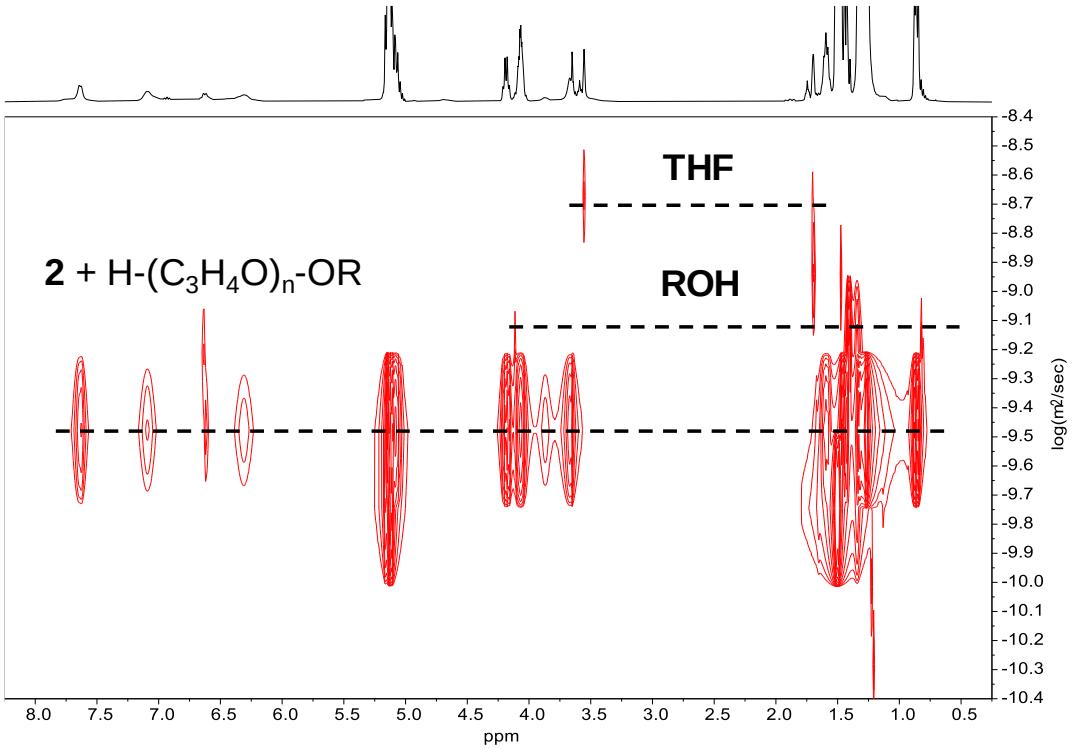

Figure S32. ^{1}H-DOSY NMR spectrum in THF-d_8 of the PLLA synthesized using **2** and ROH.

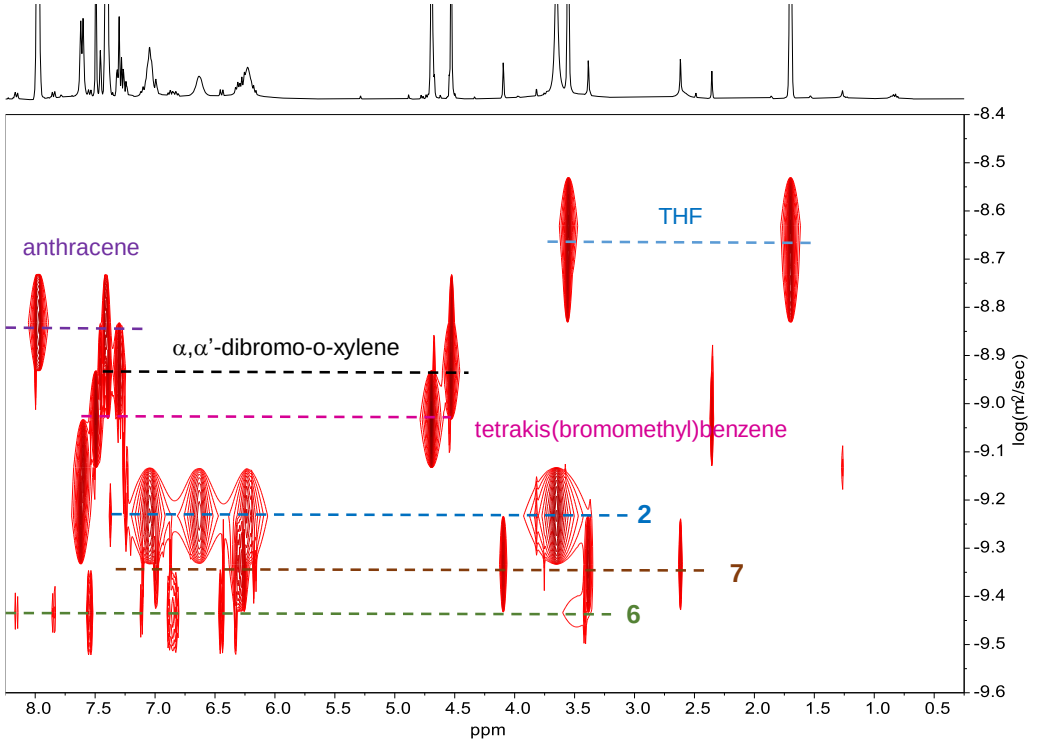

Figure S33. ^{1}H DOSY NMR spectrum of a mixture of anthracene, α,α'-dibromo-o-xylene, 1,2,4,5-tetrakis(bromomethyl)benzene, and **6** in THF-d_8.

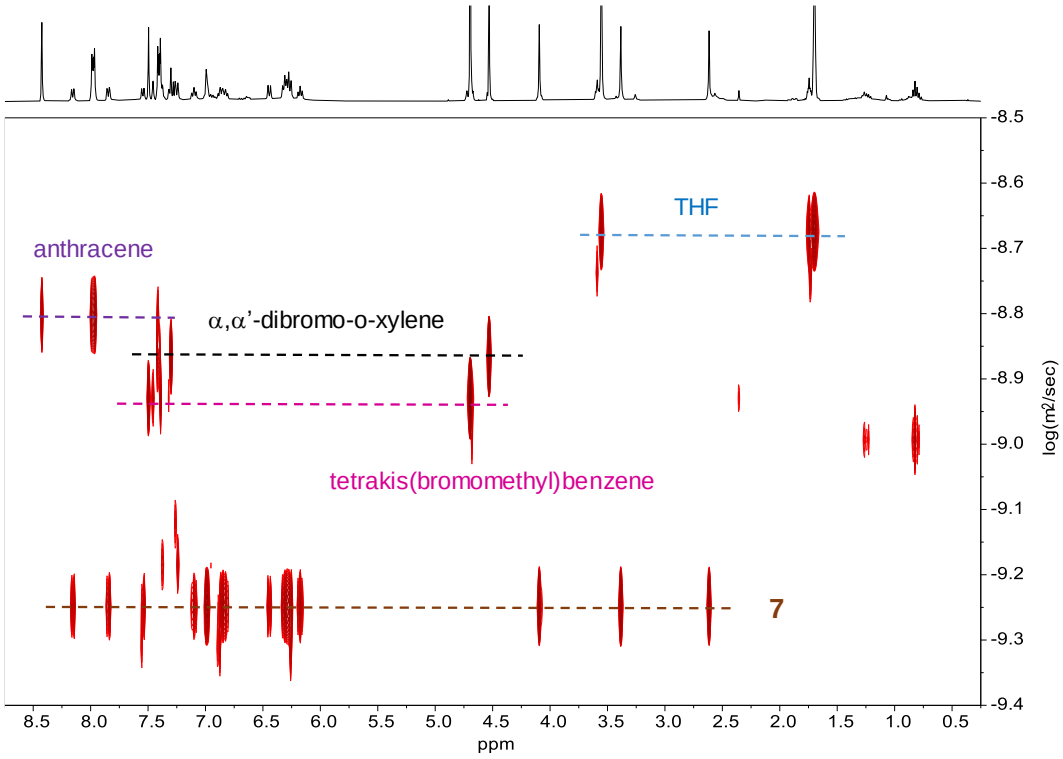

Figure S34. ^{1}H DOSY NMR spectrum of a mixture of anthracene, α,α'-dibromo-o-xylene, 1,2,4,5-tetrakis(bromomethyl)benzene, and **7** in THF-d_8.

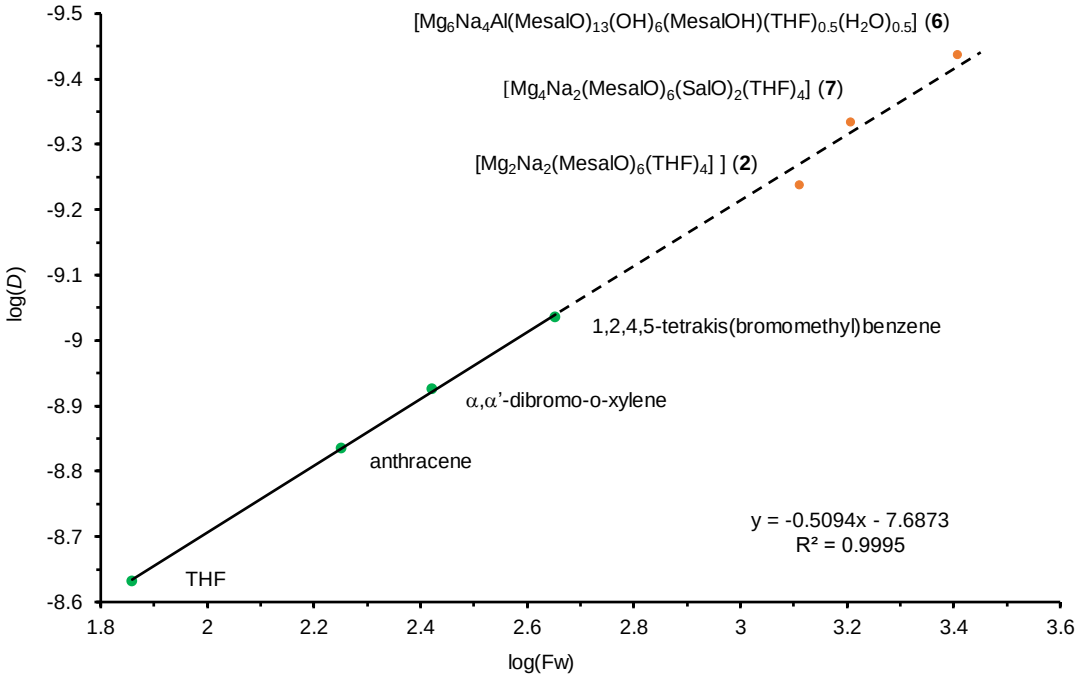

Figure S35. Plot of diffusion coefficient (log*D*) versus formula weight (log Fw) of a mixture of anthracene, α,α'-dibromo-o-xylene, 1,2,4,5-tetrakis(bromomethyl)benzene and **6** in THF-d_8.

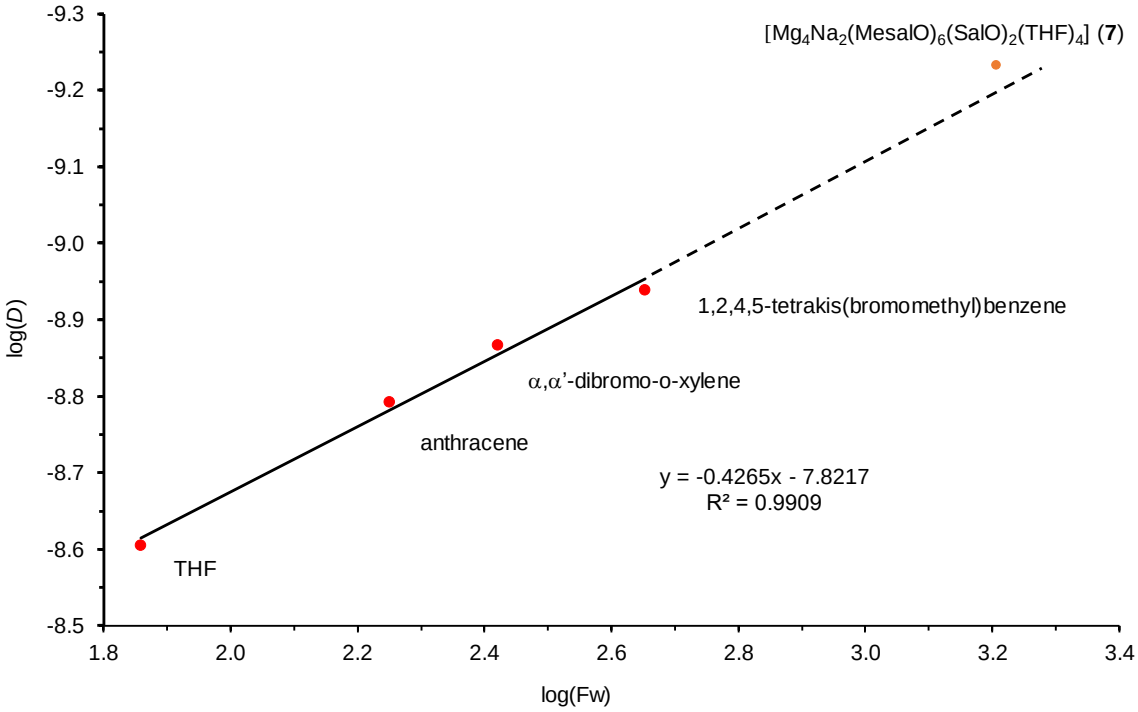

Figure S36. Plot of diffusion coefficient (log*D*) versus formula weight (log Fw) of a mixture of anthracene, α,α'-dibromo-o-xylene, 1,2,4,5-tetrakis(bromomethyl)benzene and **7** in THF-d_8.